spFRET studies of nucleosome dynamics modulated by histone modifications, histone variants and neighboring nucleosomes

Buning, R.

CHAPTER 1

Single-pair FRET experiments on nucleosome conformational dynamics

Ruth Buning and John van Noort

Based on: Biochimie, vol. 92, no.12, pp. 1729-1740, 2010

Abstract

Nucleosomes, the basic units of DNA compaction in eukaryotes, play a crucial role in regulating all processes involving DNA, including transcription, replication and repair. Nucleosomes modulate DNA accessibility through conformational dynamics like DNA breathing - the transient unwrapping of DNA from the nucleosome, repositioning of nucleosomes along the DNA, or partial dissociation. Single-molecule techniques, in particular single-pair Fluorescence Resonance Energy Transfer (spFRET), have resolved such conformational dynamics in individual nucleosomes. Here, we review the results of FRET experiments on single nucleosomes, including fluorescence correlation spectroscopy (FCS), confocal single-molecule microscopy on freely diffusing nucleosomes and widefield total internal reflection fluorescence (TIRF) microscopy on immobilized nucleosomes. The combined spFRET studies on single nucleosomes reveal a very dynamic organization of the nucleosome, that has been shown to be modulated by post-translational modifications of the histones and by DNA sequence.

1.1 Introduction

DNA in eukaryotes is condensed inside the cell nucleus by roughly an equal mass of histone proteins into a structure called chromatin. While the term chromatin was already proposed in 1882 ("the substance in the nucleus that is readily stained" [2, 3]), even before DNA was identified as the carrier of genetic information, the nucleosome was first discovered in the 1970's by electron microscopy on chromatin spilling out of ruptured nuclei [4, 5].

The nucleosome is the basic unit of chromatin: a disk of eight histone proteins with 147 bp of DNA wrapped around it. Arrays of nucleosomes are packed into higher-order structures, the details of which are still under debate. Figure 1.1 shows the hierarchical organization of chromatin at different length scales. DNA and histones are localized in the cell nucleus, and regions of higher and lower compaction can be distinguished (figure 1.1a: recent visualization of chromatin compactness using FRET). One of the first detailed images of native chromatin, spilling from ruptured nuclei (figure 1.1b), shows that it consists of fibers of ~ 30 nm in diameter. When these are disrupted, a 'beads on a string' structure appears: arrays of nucleosomes connected by short stretches of DNA. The crystal structure of the nucleosome was resolved at 7.0 Å by Richmond et al. in 1984 [6], and in 1997 at 2.8 Å resolution [7] (figure 1.1c).

All processes involving DNA, like transcription, replication and repair, take place in the chromatin environment. Besides compacting DNA, chromatin plays a major role in regulating these processes. By changing chromatin compaction, DNA-accessibility can be modulated. The control of DNA activity by the dynamics of chromatin structure has been investigated at many different levels of chromatin organization. In this review, we will zoom in on the lowest level and mainly focus on DNA dynamics within individual nucleosomes. In particular we will discuss single-molecule experiments using FRET, that have the unique capacity to directly reveal conformational dynamics of DNA inside a single nucleosome. Related to conformational dynamics of DNA inside a single nucleosome, we will also discuss DNA dynamics in assemblies of a few nucleosomes. Though regulation processes are likely to involve modulation of higher order structures as much as the modulation of nucleosome integrity and dynamics, the recent reports on single nucleosomes have laid down a framework that provides a foundation for structural understanding of the much more controversial higher-order chromatin structure.

1.2 The nucleosome

The nucleosome core particle (NCP) consists of 147 bp DNA, corresponding to ~ 50 nm, wrapped in 1.65 superhelical turns around a core of eight histone proteins

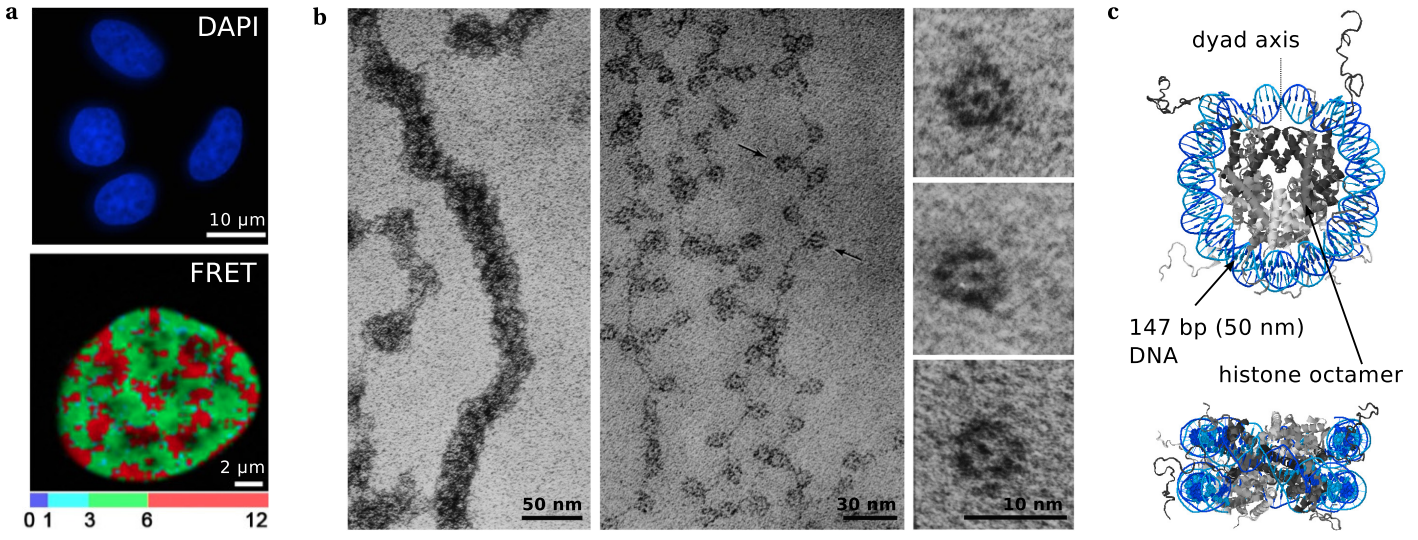

Figure 1.1 – Chromatin at different length scales. **a:** Fluorescence image of HeLa cell nuclei with DAPI stained DNA (top). All DNA of a single cell, 2 m in total, is contained in the cell nucleus of ~10 µm. FRET map of a HeLa cell nucleus with GFP/mCherry-tagged histones (bottom). High-FRET regions (red) indicate regions where the chromatin is more compacted than in low-FRET regions (green) (adapted from [8]). **b:** Electron micrograph images of native chromatin; left: chromatin spread at low ionic strength, showing a 30 nm thick fiber; middle: chromatin spread at high ionic strength, showing 'beads on a string', nucleosomes connected by stretches of DNA; right: isolated mononucleosomes (adapted by permission from Macmillan Publishers Ltd: Nature Reviews Molecular Cell Biology [3], copyright 2003. Originally published in [9–11]). **c:** Crystal structure of the nucleosome core particle (NCP) 1KX5 top- and side- view [12]. 147 bp of DNA is wrapped around an octamer of histone proteins.

[7, 13]. Two copies each of the histones H2A, H2B, H3 and H4 form the histone octamer core. Electrostatic interactions and hydrogen bonds between histones and the DNA backbone occur approximately every ten bp, at the minor groove. These 14 contact points between the histones and the DNA keep the nucleosome together. The persistence length of DNA is about 50 nm, which means that, if unconstrained, DNA is approximately straight on this length scale. Yet in the nucleosome, one persistence length of DNA is wrapped in nearly 2 full turns, rendering the nucleosome a loaded spring. A detailed discussion of the energy balance between binding and bending is given by Prinsen and Schiessel, who show that the average net binding energy per attachment point slightly exceeds one $k_B T$ ([14], [15]), allowing for extensive dynamics. *In vivo*, linker histone H1 or H5 can bind the two exiting DNA strands, stabilizing the nucleosome. Flexible N-terminal tails of the histone proteins protrude to the outside of the nucleosome and may further stabilize DNA-histone interactions. In native chromatin, 10-90 bp linker DNA connects neighboring nucleosomes.

1.2.1 Nucleosome dynamics

By letting nucleosomal DNA temporarily unwrap from the nucleosome, or by regulating the position and density of nucleosomes along genomic DNA, nucleosomes play an essential role in regulating DNA accessibility, and with this transcription. Spontaneous (thermal) fluctuations can lift steric occlusion, providing access to DNA target sites for DNA-processing enzymes that are buried inside nucleosomes. Such fluctuations include (see figure 1.2) [16, 17]: DNA breathing, the transient unwrapping of nucleosomal DNA; H2A-H2B dimer release; and thermal repositioning of the histone octamer with respect to the DNA (sliding). Access to nucleosomal sites can also be catalyzed by remodeling enzymes that use ATP hydrolysis to change the position, structure or composition of nucleosomes.

The N-terminal histone tails may play an important role in regulating nucleosome dynamics. They interact with the nucleosomal DNA by binding or constraining it. The histone tails can also mediate interactions between nucleosomes, thereby organizing higher-order chromatin structure [18, 19].

Post-translational modifications of the histones, like acetylation, methylation, ubiquitylation and phosphorylation of amino acid residues, influence transcription activity. Although nucleosomes were only discovered in the 1970's, that chromatin consisted of nucleic acids and histones was known almost a century before. Already in 1964, it was shown that histone modifications and chromatin transcription are associated [20]. Histone modifications can change the charge of amino acid residues, and thereby alter electrostatic interactions. It is therefore likely that these modifications modulate DNA accessibility at the nucleosome level. Many post-translational modifications on both the histone tails and the globular domain have been mapped [21].

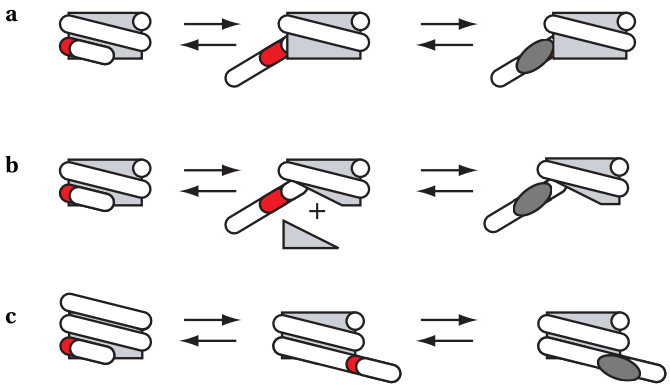

Figure 1.2 – Possible mechanisms for spontaneous site exposure of nucleosomal DNA, providing access to recognition sites (red) for DNA-binding proteins (dark grey). **a:** DNA breathing, **b:** H2A/H2B dimer release, **c:** thermal repositioning.

Nonspecific acetylation of lysine residues on histones is expected to weaken electrostatic interactions between mainly the histone tails and DNA by neutralizing a positive charge. Also, several specific modifications have been associated to the regulation of chromatin dynamics. Especially acetylation of H4 K16, a lysine on the tail of H4 that presumably interacts with the neighboring nucleosome, has been implicated to inhibit the formation of higher-order chromatin structure [22, 23]. The ensemble of post-translational modifications on the histone tails have been proposed to provide a 'histone code', that may recruit specific protein factors involved in active remodeling of nucleosomes [24].

In the globular domain, acetylation of H3 K56 is most extensively studied in relation to transcription activity. Numerous reports show that it plays a role in the regulation of DNA repair and replication, transcription and chromatin assembly [21]. This amino acid is located close to the nucleosome exit, where the histone contacts the nucleosomal DNA. It is therefore expected to modulate access to the nucleosomal DNA via DNA breathing.

The first study of DNA dynamics within nucleosomes was reported by Polach and Widom in 1995 [25]. They probed the accessibility of nucleosomal DNA by measuring digestion rates of restriction enzymes as a function of the position of the restriction site inside the nucleosome. Even sites buried far inside the nucleosome are digested, albeit with a lower occurrence. The equilibrium constants for DNA breathing can be determined indirectly from the digestion rates, though correct interpretation of such data is non-trivial [15].

In the last decade, single-molecule biophysics techniques have been applied to study nucleosome and chromatin dynamics. single-molecule experiments reveal co-

existing subpopulations that would otherwise remain obscured by the ensemble average, and allow to probe kinetic processes directly. single-molecule force spectroscopy has been used to probe DNA unwrapping induced by force (for a review, see [26]). Here we will discuss FRET, that has the sensitivity to probe spontaneous unwrapping, even in individual nucleosomes. In that case it is referred to as single pair-FRET (spFRET).

1.3 FRET

Förster/Fluorescence Resonance Energy Transfer is a process in which energy is transferred non-radiatively from a donor molecule (D) to an acceptor molecule (A) [27]. The transferred energy can be emitted as acceptor fluorescence, with a wavelength that is longer than the donor fluorescence. The efficiency of energy transfer is defined as the amount of energy that is transferred from the donor to the acceptor, divided by the total amount of energy absorbed by the donor. The FRET efficiency E depends strongly on the distance between the fluorophores (see also figure 1.3a):

$$E = \frac{1}{1 + \left(\frac{R}{R_0}\right)^6}, \tag{1.1}$$

where R is the distance between the donor and the acceptor, and R_0 the Förster radius, or the distance at which the FRET efficiency is reduced to 0.5. R_0 is typically around 5 nm. This makes FRET an ideal tool to study conformational dynamics of the nucleosome, which has a radius of ~ 5 nm. A detailed discussion of FRET and its biological applications can be found in [28–30].

E can be experimentally determined from the donor and acceptor fluorescence intensities upon excitation of the donor:

$$E = \frac{I_A}{I_A + \gamma I_D}, \tag{1.2}$$

where I_A and I_D are the measured acceptor and donor fluorescence intensities, respectively, and γ is a correction factor containing the donor and acceptor quantum yield and detector efficiencies. When FRET is used for absolute distance measurements, I_A and I_D need to be corrected for direct acceptor excitation and crosstalk between the donor and acceptor channels. A detailed description of how to apply these corrections, as well as how to determine γ, is given by [31]. To translate the corrected E into an absolute distance via equation 1.1, the Förster radius R_0 needs to be known:

$$R_0^6 = \frac{9 \ln 10 \, \Phi^D \kappa^2 J(\nu)}{128 \pi^5 N_A n^4} = \left(8.785 \times 10^{-25}\right) \Phi^D \kappa^2 n^{-4} J(\nu), \tag{1.3}$$

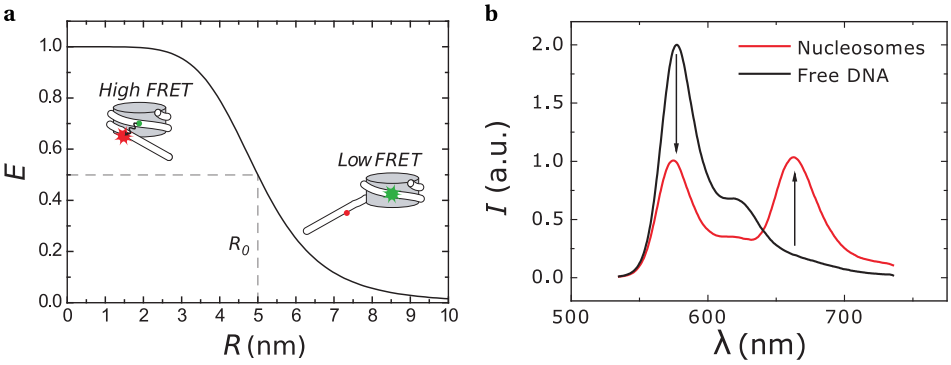

Figure 1.3 – **a:** FRET efficiency E as a function of the distance between the dyes with a Förster radius R_0 of 5 nm. Since the radius of the nucleosome is ~5 nm, the FRET efficiency for labels attached to the DNA will decrease from one to zero for DNA breathing events; **b:** Bulk fluorescence spectrum upon donor excitation for free DNA (black) and for reconstituted nucleosomes (red).

where Φ^D is the donor emission quantum yield in absence of the acceptor, $J(\nu)$ the spectral overlap integral, n the refractive index of the medium, and κ the orientation factor for dipole-dipole coupling. The relative orientation of the dyes with respect to each other determines κ^2, the value of which can vary between 0 and 4. It is often assumed that the D and A dipole moments are free to rotate in all directions on a timescale much faster than their radiative lifetimes. In this case, the geometric average of the angles can be used and $\kappa^2 = 2/3$. However, in many cases fluorophores are restricted in their movement by the presence of the molecule to which they are attached. When FRET is only used to probe dynamics between different conformational states, changes in E, instead of absolute values of R, are of interest. In this case, γ in equation 1.2 can be assumed to be 1, and the uncorrected E is called the *proximity ratio*.

Deliberately detuning the proximity ratio can be applied to optimally separate two states close in FRET efficiency [32]. Here, the factor γ is manipulated by changing the donor and acceptor detection efficiencies.

Note that the limited fluorescence intensity from single fluorophores results in a relatively large contribution of shot noise in typical spFRET experiments, resulting in a relatively poor signal-to-noise ratio of E, making accurate determination of E challenging.

1.4 Reconstitution of nucleosomes

Nucleosomes can be assembled from DNA and purified histones. Simply mixing these two together at physiological salt conditions however results in the formation of non-

specific aggregates. *In vivo*, nucleosome assembly is therefore assisted by histone chaperones. *In vitro*, aggregation is prevented by reconstituting nucleosomes via salt-gradient dialysis. At high salt (typically 2 M monovalent salt), the histone octamers dissociate from the DNA. At 1.2-1.0 M salt, the $(H3\text{-}H4)_2$ tetramer binds to the DNA. Subsequently, at ~700 mM salt, the two H2A-H2B dimers dock onto the tetramer and constrain the ends of the DNA.

Typically, small fluorophores like Cy3 or Cy5 are attached to a DNA base via a 1-2 nm flexible carbon linker, ensuring rotational freedom of the dyes. Alternatively, a donor or acceptor fluorophore can be attached to one of the histones. Since there are two copies of each histone in the nucleosome, histone-labeled nucleosomes can contain no, one, or two copies of the same fluorophore, depending on the labeling stoichiometry, which may complicate quantitative interpretation of the FRET value. For accurate interpretation of the observed FRET efficiencies, a well defined positioning of the dyes is crucial. Therefore, the DNA template usually contains a strong nucleosome positioning element, for example 5S rDNA or the 601-positioning sequence [33]. Fluorescent labels can be incorporated in the nucleosomal DNA through a PCR with fluorescently labeled primers. A detailed protocol for designing and reconstituting mononucleosomes can be found in [34]. Figure 1.3b shows the fluorescence spectrum upon donor excitation for Cy3B- and ATTO647N- labeled unreconstituted DNA and nucleosomes after reconstitution. The spectrum shows that, in the reconstituted nucleosomes, the donor and the acceptor are positioned close enough to each other to show efficient FRET. However, the bulk spectrum hides all conformational dynamics, non-stoichiometric labeling and incomplete reconstitution, which can be prominent under typical experimental conditions.

Figure 1.4 ***(facing page)*** – **a-f:** Selection of nucleosome constructs used for FRET experiments. The NCP is shown, with the bases or amino acids to which the dyes are attached indicated in green (D) or red (A); **a** and **b:** constructs used by Li et al. [35, 36]; **c** and **d:** constructs used by Gansen et al. [32, 37, 38]; **e:** construct used by Tomschik et al. [39]; **f:** construct used by Koopmans et al. [40–42]; **g:** Schematic drawing of the nucleosome. The distance between the bases is calculated via $R_{\text{bases}} = \sqrt{R_{2D}^2 + H^2}$. The distance between the dyes is approximated by taking $R = R_{\text{bases}} + \Delta R$; **h:** Calculated FRET efficiency as a function of the length of unwrapped DNA based on the geometry depicted in g), for four of the constructs shown in a). Input values are: $R_{\text{nuc}} = 4.18$ nm, $H = 2.8$ nm [7], Förster radius for the specific FRET pair used = 5.5-6.5 nm, nm/bp = 0.34. The thick lines represent calculations with ΔR corresponding to the reported FRET efficiencies for fully wrapped nucleosomes. The shaded areas indicate the extremes for excursions of the dyes corresponding to $\Delta R \pm 1$ nm. Vertical dotted lines indicate contact points between the DNA and the histones [7].

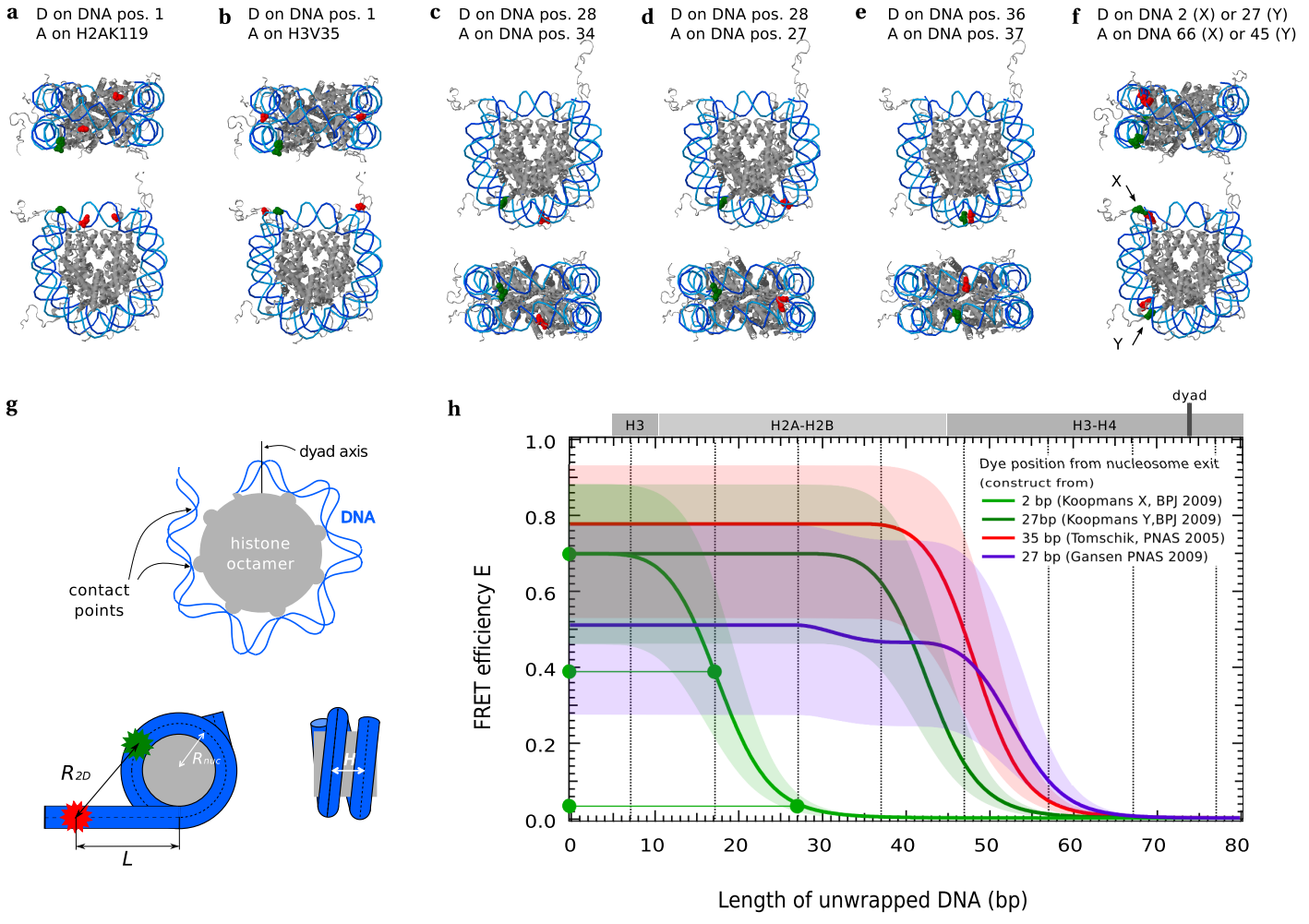
a
D on DNA pos. 1
A on H2AK119
b
D on DNA pos. 1
A on H3V35
c
D on DNA pos. 28
A on DNA pos. 34
d
D on DNA pos. 28
A on DNA pos. 27
e
D on DNA pos. 36
A on DNA pos. 37
f
D on DNA 2 (X) or 27 (Y)
A on DNA 66 (X) or 45 (Y)
X
Y
g
dyad axis
DNA
histone
octamer
contact
points
R2D
RDA
L
h
dyad
H3
H2A-H2B
H3-H4
Dye position from nucleosome exit
(construct from)
2 bp (Koopmans X, BPJ 2009)
27bp (Koopmans Y,BPJ 2009)
35 bp (Tomschik, PNAS 2005)
27 bp (Gansen PNAS 2009)
FRET efficiency E
Length of unwrapped DNA (bp)

1.4.1 Relation between FRET efficiency and length of unwrapped DNA

A variety of different label positions have been reported. In order to compare the results and to deduce generic dynamic properties of nucleosomes, we need to carefully consider the geometries of the FRET-labeled nucleosomes. Figures 1.4a-f show a selection of reported nucleosome constructs. We can estimate how the FRET efficiency evolves when the nucleosomal DNA unwraps via a simple geometric model, schematically drawn in figure 1.4g. The dyes are attached to the DNA by a 1-2 nm flexible linker. Their separation is roughly estimated by calculating the distance between the DNA bases to which they are attached, plus an additional distance ΔR that represents the length of the flexible linker. ΔR is estimated from the reported FRET efficiencies for fully wrapped nucleosomes. Figure 1.4h shows the resulting FRET efficiency as a function of the length of unwrapped DNA for four different nucleosome constructs. DNA has to unwrap as far as ~ 30 bp beyond the label positions to lose FRET completely. If we assume that DNA unwraps from the nucleosomes in discrete steps that correspond to the contact points between the DNA backbone and the histone octamers, it follows that one or two intermediate states could exist as well. Whether the intermediate FRET efficiencies of these states can be distinguished from the high and low FRET states depends on the label positions. However, in many cases it is sufficient to describe DNA breathing with a two-state model where the nucleosome is either in a closed conformation (high E) or an open conformation (low E).

1.5 spFRET techniques

single-molecule techniques have allowed to measure a wealth of information that would remain obscured in the ensemble average: rates and lifetimes of dynamic processes and conformational heterogeneity. Specific sub-populations can be selected, to investigate them independently, or for example to exclude inefficient labelled species or not-reconstituted DNA. To detect the fluorescence of single molecules, it is crucial to reduce the background fluorescence originating from other molecules. Common single-molecule fluorescence techniques applied to nucleosomes include confocal microscopy to measure nucleosomes diffusing freely in solution, and widefield total internal reflection (TIRF) microscopy on nucleosomes immobilized to a surface. A schematic layout of both setups is shown in figure 1.5.

1.5.1 Confocal microscopy

With confocal microscopy, the excitation laser is focused to a femtoliter-sized excitation volume. Opposed to scanning confocal microscopy, where an image is created

by scanning the excitation volume through the sample, here time traces of the fluorescence intensity in the stationary laser focus are collected. Each nucleosome that enters the excitation volume gives a burst of fluorescence. The emitted fluorescence is collected by the objective and background fluorescence is rejected by a pinhole. Photons emitted by the donor and by the acceptor are separated and detected by single-photon counting devices like avalanche photodiodes (APDs). The time resolution can be as good as ps-μs.

When the concentration is low enough, typically $10-100$ pM, only a single nucleosome at a time will be in the excitation volume. In this case, burst analysis can resolve single-nucleosome FRET efficiencies, yielding the distribution of nucleosome conformations in the sample. The observation time per nucleosome is limited to the diffusion time through the excitation volume, typically a few ms.

The temporal fluctuations in fluorescence intensity can also be analyzed in terms of correlation times. Time traces of photon intensities are generally measured at low concentrations, but not necessarily at the level of single molecules. The normalized correlation function is defined as:

$$G_{1,2}(\tau) = \frac{\langle I_1(t)\, I_2(t+\tau)\rangle}{\langle I_1(t)\rangle \langle I_2(t)\rangle} - 1, \tag{1.4}$$

where $I_1(t)$ and $I_2(t)$ are the photon intensities of the channels of interest (D or A or a combination), and τ is the lag time. If $I_1 = I_2$, $G(\tau)$ is an autocorrelation, and if $I_1 \neq I_2$, $G(\tau)$ is a cross-correlation.

The fluorescence fluctuations can arise from processes like diffusion and fluorophore photophysics, but also from FRET fluctuations caused by conformational dynamics. The measured correlation function $G(\tau)$ is the product of contributions from these independent processes: $G(\tau) = G_{\text{diff}}(\tau) \times G_{\text{kin}}(\tau)$. When the timescale of conformational dynamics is much longer than the residence time, diffusion dominates the correlation curve, masking the dynamics almost completely.

1.5.2 Widefield TIRF

When nucleosomes are immobilized to the surface of a microscope slide, the observation time per single nucleosome is only limited by bleaching of the fluorophores. Though confocal microscopy can still be used, more often widefield excitation is chosen. A reduction of the background fluorescence is obtained by Total Internal Reflection Fluorescence (TIRF) microscopy, using the evanescent field created by directing the excitation laser to the sample under an angle greater than the critical angle via a prism or the objective. The evanescent field excites only those fluorophores within ~ 100 nm from the surface. Fluorescence is collected by the objective, separated into a donor and acceptor channel using dichroic mirrors, and detected on a CCD cam-

era. The time resolution, given by the readout-time of the CCD camera, is typically ~ 10 ms, limited by the number of photons per frame that is necessary for a reasonable signal-to-noise ratio. Multiple nucleosomes immobilized to the surface can thus be measured in parallel. The observation time for individual nucleosomes can be minutes long, depending on the photostability of the fluorophores. Because of the long observation time, it is even possible to perform multiple experiments on an individual nucleosome, e.g. by varying the buffer conditions during the observation.

The presence of the surface can however form a major obstacle in these studies. As nucleosomes tend to stick nonspecifically, special measures have to be taken to prevent nucleosome-surface interactions. Koopmans et al. showed that polymer-coating the surface with 6-arm polyethylene glycol (starPEG) reduces surface artifacts effectively [41].

1.5.3 Alternating Laser Excitation

spFRET experiments are particularly sensitive to artifacts related to the photophysical stability of the fluorescent labels. Photobleaching is the irreversible loss of fluorescence and limits the observation time of the fluorophore. A fluorophore typically emits ~ 10^5 photons before bleaching. Photoblinking is a reversible loss of fluorescence, where the fluorophore exists transiently in a dark state. When the acceptor fluorophore blinks, this can be mistaken for a loss of FRET, and therefore as nucleosome dynamics. Removing oxygen from the sample by using 'oxygen scavenging systems' and adding triplet state quenchers like trolox increases the photostability of the dyes.

Figure 1.5 ***(facing page)*** – Examples of single-pair FRET microscopes. **a:** Widefield TIRF microscope. DM, dichroic mirror; AOTF, Acousto Optical Tunable Filter; EF, Emission Filter; CCD, Charge Coupled Device. TIR excitation is achieved by displacing the excitation beams relative to the optical axis. The resulting fluorescence (orange) from immobilized molecules is collected by the objective, and filtered through an emission filter. Donor (green) and acceptor (red) fluorescence are simultaneously imaged on separate areas of the CCD chip using a dichroic mirror wedge. **b:** Fluorescence microscope with confocal geometry. AOM, Acousto Optical Modulator; PH, Pinhole; SPAD, Single-Photon Avalanche Diode. The resulting fluorescence from freely diffusing molecules in the excitation volume is collected by the objective, filtered through an emission filter, and spatially filtered through a pinhole. Donor and acceptor fluorescence are imaged on different SPADs using a dichroic mirror. In both **a** and **b**, a red and a green laser are alternated (green and red boxes) at a frequency that is synchronized to the fluorescence detection. Alternating Laser Excitation (ALEX) allows to simultaneously determine the FRET efficiency E and the label stoichiometry S for every particle. **c:** 2D E, S-histogram, revealing the presence of four different populations: donor- (D) or acceptor- (A) only species (due to incomplete labeling or photobleaching or –blinking), and doubly labeled species with high or low FRET. The first two can be excluded from the analysis.

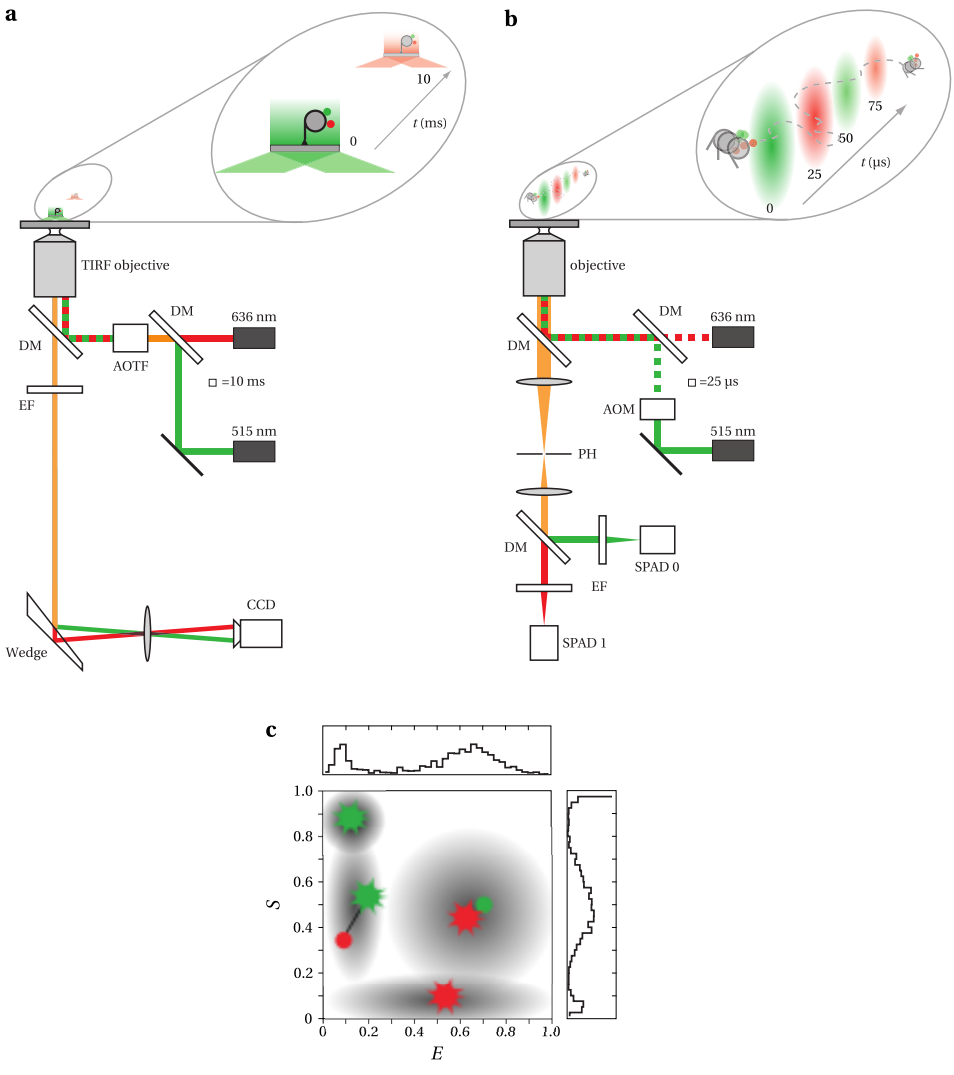
a
10
t (ms)
0
P
TIRF objective
DM
636 nm
DM
AOTF
EF
=10 ms
515 nm
CCD
Wedge
b
75
50
25
t (µs)
0
objective
DM
636 nm
DM
=25 µs
AOM
515 nm
PH
DM
SPAD 0
EF
SPAD 1
c
1.0
0.8
0.6
0.4
0.2
0
S
0
0.2
0.4
0.6
0.8
1.0
E

A powerful tool to monitor the presence and integrity of both labels is Alternating Laser EXitation (ALEX), introduced by Kapanidis et al. [43]. The laser to excite the donor is rapidly alternated by a laser that directly excites the acceptor. This second laser monitors the presence and integrity of the acceptor, and reveals blinking events. With ALEX, the label stoichiometry S can be determined simultaneously with the FRET efficiency E:

$$S = \frac{I_A^{Dex} + I_D^{Dex}}{I_A^{Dex} + I_D^{Dex} + I_A^{Aex}},$$

where I_A^{Dex} and I_D^{Dex} are the acceptor and donor intensities when excited at the donor excitation wavelength, and I_A^{Aex} the acceptor intensity when excited directly at the acceptor excitation wavelength. Nucleosomes with only a donor will have $S = 1$, and acceptor-only species $S = 0$. Properly folded nucleosomes with both fluorescent labels will have a high E and a S close to 0.5. Unwrapped nucleosomes and free DNA will have a low E and S close to 0.5 (see figure 1.5). ALEX allows to distinguish subpopulations based on label stoichiometry, and select the ones of interest or follow changes in population sizes in time. Thus ALEX can be particularly useful for spFRET experiments in nucleosomes, where eliminating artifacts due to photoblinking and D-only species is crucial for the correct interpretation of DNA breathing dynamics.

Next to the fluorescence intensity of the D and A labels, other information can be obtained, for example fluorescence lifetime and anisotropy. The simultaneous detection and analysis of these parameters, known as Multiparameter Fluorescence Detection (MFD) [44], allows to resolve heterogeneity in the sample via photophysical behavior.

1.6 DNA breathing studied with spFRET

Li & Widom investigated the conformational equilibrium of FRET-labeled nucleosomes under varying salt concentrations and in the presence of site-specific DNA binding proteins with bulk spectroscopy [35] (see figure 1.6 and 1.4a and b). Salt-induced loss of FRET shows that the equilibrium between wrapped and partially unwrapped states depends on the salt concentration. The resulting equilibrium constant (unwrapped/wrapped nucleosomes) under physiological conditions ($\sim 0.1 - 0.15$ M ionic strength), is $K_{eq} = 0.02 - 0.1$. This means a nucleosome is partially unwrapped for 2-10 % of the time. Addition of LexA decreases the FRET efficiency, and drives the equilibrium to the unwrapped state, inhibiting rebinding of the DNA to the octamer. These bulk measurements set the stage for spFRET applications that aim at resolving the rates of (un)wrapping and possible heterogeneities in the nucleosome populations.

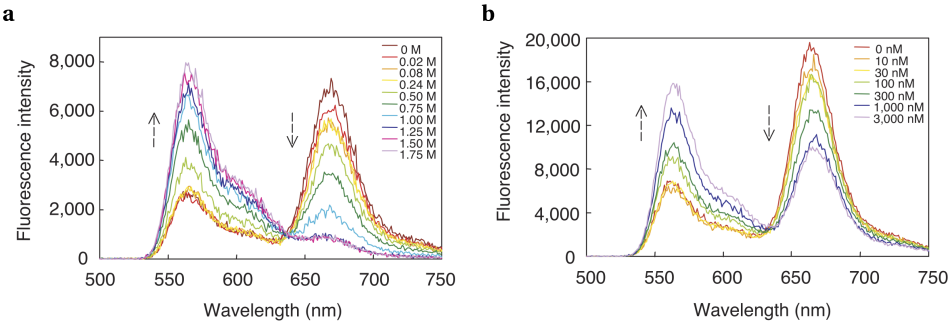

Figure 1.6 – **a:** FRET decrease upon increasing [NaCl], indicating unwrapping of the nucleosomal DNA; **b:** Titration of LexA to nucleosomes with a LexA recognition site 15 bp inside the nucleosomal DNA. Unwrapping of nucleosomal DNA upon specific protein binding. (Adapted by permission from Macmillan Publishers Ltd: Nature Structural and Molecular Biology [35], copyright 2004).

Li et al. performed FCS and stopped-flow FRET experiments on mononucleosomes (construct of figure 1.4b) freely diffusing in solution [36]. To resolve DNA breathing, its contribution has to be extracted from the correlation curve. A common way to do this is to measure an additional sample with only the diffusion, e.g. a D-only sample. The thus obtained diffusion correlation curve can be divided out, leaving the kinetics contribution. The resulting lifetimes are 250 ms and 10-50 ms for the closed and the open states, respectively. This method is very sensitive to the concentrations of both sample and reference. Also, by changing samples one risks introducing artifacts associated with changes in the observation volume. Therefore, Torres & Levitus developed a different approach to obtain kinetics information from correlation curves [45]. They show that from a single sample, the ratio of any two correlation curves cancels out the diffusion term. Reanalysis of the same data led to on/off times of 1.2 s and 50 ms, respectively (figure 1.7).

DNA breathing dynamics measured with TIRF microscopy on immobilized nucleosomes was first reported by Tomschik et al. [39]. They observed long-range DNA breathing of more than 35 bp (figure 1.4e), which they refer to as 'opening'. The reported on- and off-times are 2-5 s and 100-200 ms, respectively, depending on the ionic strength. These results were later re-interpreted as photoblinking of the acceptor [46]. In a later study by Koopmans et al., immobilized nucleosomes with the label positions at the nucleosome exit were measured using ALEX (figure 1.4f) [40]. It was shown that trolox [47] suppressed acceptor blinking. Another issue that effects breathing is the presence of the surface. Of all the immobilized nucleosomes, only 10 % appeared intact, with both a donor and acceptor label and high FRET, and only 3 % of these show FRET fluctuations related to DNA breathing. Apparently the presence of the surface

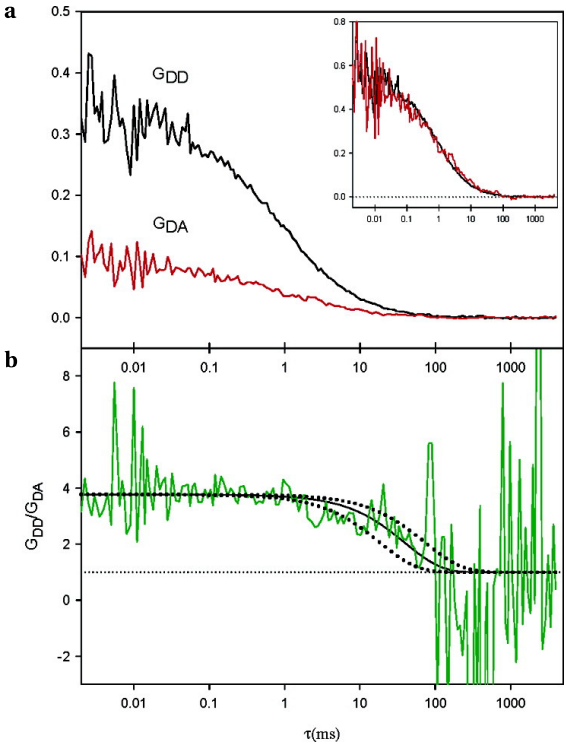

Figure 1.7 – **a:** Experimental donor-autocorrelation $G_{DD}(\tau)$ (black) and donor-acceptor crosscorrelation $G_{DA}(\tau)$ (red) FCS curves, from donor- and acceptor labeled nucleosomes (inset: normalized G_{DD} and G_{DA}); **b:** The ratio between the two divides out the contribution of diffusion and leaves the contribution of conformational dynamics. (Reprinted with permission from [45]. Copyright 2007 American Chemical Society.)

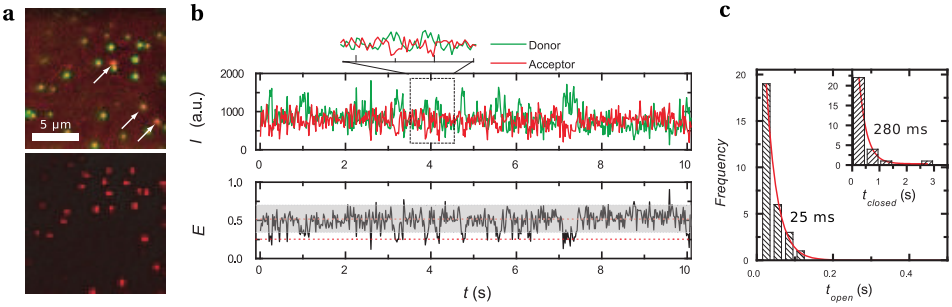

Figure 1.8 – Dynamics of nucleosomes immobilized on a starPEG surface. **a:** single-molecule fluorescence image of immobilized nucleosomes. Top: false color representation of donor and acceptor channel images, excited at 514 nm. The arrows point at molecules that featured high FRET efficiency. The majority of the molecules however did not show FRET and appears in green. Bottom: the same field of view excited at 636 nm, allowing for unambiguous identification of acceptor fluorophores (adapted with permission from Springer Science+Business Media [40]). **b:** Fluorescence intensity time trace (top) and corresponding FRET efficiency time trace (bottom). The FRET efficiency fluctuated between a high and a low FRET state, corresponding to a closed and an open nucleosome conformation, respectively. The grey bar indicates a 96 % confidence interval for the photon and instrument noise. **c:** Histograms of the lifetime of the open and closed (inset) state. The solid lines are exponential fits to the data, yielding lifetimes of 25 ms for the open state and of 280 ms for the closed state (copyright Wiley-VCH Verlag GmbH & Co. KGaA. Reproduced with permission from [41])

impairs nucleosome integrity and probably also the dynamics of DNA breathing, despite surface passivation with polyethylene glycol (PEG). In a subsequent study, nucleosome integrity was investigated in relation to immobilization on either BSA, PEG, starPEG (6-arm PEG that forms cross-links), and in polymer gels [41]. StarPEG coating prevented nonspecific tethering most effectively, leaving 25 % of the immobilized nucleosomes intact. Time traces with 10 ms time resolution show lifetimes of closed and open states of 280 ms and 25 ms, respectively (figure 1.8). This is in good agreement with Li et al. [36], while the closed state lifetime is short compared to the 1.2 s reported by Torres and Levitus [45].

Gansen et al. investigated the effect of salt concentration, nucleosome concentration and crowding agents on nucleosome stability [37] by burst analysis of freely diffusing single nucleosomes (figure 1.4c and d). When working with low concentrations, essential to observe individual nucleosomes, they show that nucleosomes dissociate at low concentrations and at high salt (NaCl), but that ~ 0.2 mg/ml BSA maintains nucleosome integrity for up to 300 mM NaCl. In fact, BSA is more effective then adding unlabeled nucleosomes, a common way to increase the nucleosome concentration while keeping the labeled nucleosome concentration low. A thorough quantitative analysis

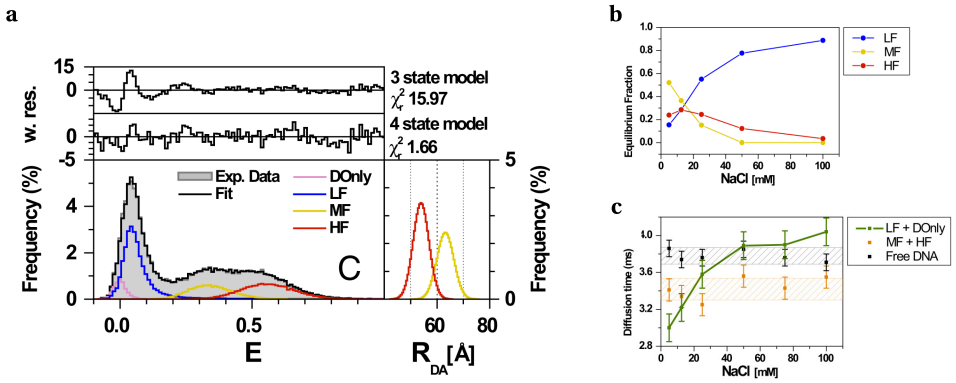

Figure 1.9 – **a:** FRET efficiency histogram of nucleosomes in 25 mM NaCl. Probability Distribution Analysis shows 4 different species: D-only, Low FRET (LF), medium FRET (MF), and high FRET (HF); **b:** Equilibrium fractions of LF, MF, and HF as a function of NaCl concentration; **c:** FCS correlation times of the subpopulations as a function of NaCl concentration. (Reproduced from [38].)

of FRET histograms of mononucleosomes is presented in [38]. Probability distribution analysis (PDA), combined with multiparameter fluorescence detection (FRET efficiency, lifetimes, and anisotropy) and FCS reveals at least four different subspecies with different FRET efficiency: three nucleosome species, with high (~ 0.5), medium, (~ 0.32) or low (close to zero) FRET, and a D-only population. Salt dependent stability analysis of these species identified these populations as intermediates in nucleosome disassembly. Based on these observations, a model is proposed for stepwise dissociation: first unwrapping from the ends, than dimer loss, and finally complete dissociation (figure 1.9).

In [42], Koopmans combined spFRET, ALEX, Polyacrylamide Gel Electrophoresis (PAGE) and FCS to resolve conformational heterogeneity of mononucleosomes with labels positioned at both DNA exits and 27 bp inside (figure 1.4f). Burst analysis of nucleosomes with different label positions reveals that transient DNA unwrapping occurs progressively from both ends, while nucleosomes remain stably associated. Equilibrium constants for breathing dynamics depend on the position in the nucleosome: $K_{eq} = 0.2 - 0.6$ at the nucleosome ends, and ~ 0.1 for 27 bp inside. Also it is shown that 50-100 mM monovalent salt promotes both reversible nucleosome breathing kinetics and irreversible nucleosome disassembly at low nucleosome concentrations (100-200 pM). For the first time, FCS was applied on selected bursts. By selecting a specific subpopulation, diffusion times can be related to the hydrodynamic radius of this specific population (figure 1.10).

Overall, bulk and single-molecule FRET measurements have shed light on the con-

formational dynamics of canonical nucleosomes. The approaches agree on the characteristic equilibrium constant between wrapped and unwrapped states, showing that nucleosomes are open 10 – 20 % of the time. spFRET experiments have the advantage that they reveal much more detailed information on nucleosome dynamics, such as transition rates and conformational heterogeneities. Multiple subpopulations have been distinguished, allowing the selection of specific populations of interest. Within these populations, FRET distributions reveal the presence of multiple states. The transition rates between the open and the closed conformation have been determined, resolving a lifetime of the open state of ~ 25 ms.

1.7 DNA sequence effects

Having established the canonical dynamic breathing of DNA, spFRET also provides unique possibilities to reveal more subtle effects that are responsible for modulation of DNA accessibility. Nucleosome constructs for spFRET experiments have so far been reconstituted on strong nucleosome positioning sequences. DNA sequence itself may influence nucleosome stability and DNA breathing dynamics. Gansen et al. compared 601 and 5S rDNA positioning sequences with spFRET on freely diffusing nucleosomes [32]. The 5S rDNA nucleosome is more destabilized by salt and dilution than nucleosomes based on the 601 positioning sequence.

Kelbauskas et al. compared nucleosomes with 5S, MMTV, and GAL10 DNA, the last two derived from promotor regions [48, 49]. Bulk FRET and FCS experiments in 3 % agarose gels on nucleosomes with FRET labels at the nucleosome exit or ~ 30 bp inside the nucleosome show enhanced dynamics in nucleosomes based on DNA from promotor regions compared to 5S DNA. The destabilization they observe at sub-nM concentrations is only pronounced for nucleosomes with labels at the nucleosome exit, suggesting that the destabilization is caused by H2A-H2B dimer release. The resulting open/closed times are 34/41, 58/40 and 82/36 ms for 5S, MMTV, GAL10 DNA based nucleosomes, respectively.

Thus nucleosome stability is directly linked to the affinity of the sequence to the octamer, and it is likely that DNA sequences that have a lower affinity exhibit more pronounced DNA breathing. This may help to direct nucleosomes to preferred positions along the genome.

1.8 Histone modifications

With the advent of spFRET experiments on nucleosomes, the link between histone modifications and nucleosome integrity and conformational dynamics can be directly investigated. Gansen et al. show that nonspecific chemical acetylation of histone oc-

tamers decreases nucleosome stability by opening the nucleosome structure starting at the DNA ends by comparing the FRET distributions for nucleosomes with FRET labels at the DNA exit and with FRET labels 40 bp inside the nucleosome [38].

Specific acetylation of H3 K56, in the globular core, is expected to enhance DNA breathing. Neumann et al. developed a method to produce stoichiometric site-specific acetylated recombinant histones [50]. To investigate the effect of histone acetylation at H3 K56 on DNA breathing we compared nucleosomes reconstituted with recombinant xenopus histones without modifications, and recombinant Xenopus histones with acetylation at H3 K56. The FRET distributions were determined for both end-labeled and internally labeled nucleosomes (see figure 1.4f) using ALEX and confocal microscopy on freely diffusing nucleosomes. 13 % of the unmodified nucleosomes unwrap for 30 bp or more, and 11 % unwrap for at least 60 bp (figure 1.11). Acetylation at H3 K56 doubles the fraction that is unwrapped by 30 bp or more to 28 %, and increases the fraction that unwraps at least 60 bp with 3 % to 14 %. The FRET efficiency of the high-FRET population decreases upon acetylation. Taken together, acetylation at H3 K56 increases DNA breathing of the first ~30 bp 7-fold but hardly affects unwrapping further into the nucleosome. H3 K56 is well positioned to regulate DNA breathing, due to its position close to the exit of the nucleosome. Other modifications may have an equally important effect on enhancing or reducing DNA dynamics in the nucleosome.

1.9 Nucleosome remodeling

spFRET experiments are not only informative for quantifying DNA dynamics intrinsic to the nucleosome, they are also very well suited to probe the kinetic pathway of nucleosome remodeling.

Yang and Narlikar described a FRET based assay to follow real-time changes in

Figure 1.10 ***(facing page)*** – **a:** DNA and nucleosomes in a 5 % polyacrylamide gel. DNA and nucleosomes end up at different positions in the gel. The nucleosome band shows FRET when excited at 530 nm (orange color). The nucleosome band is directly placed on the confocal microscope setup. On the right a fluorescence time trace showing bursts of single nucleosomes. **b:** Results from burst analysis of nucleosomes with labels in position X (see figure 1.4f). Left: E,S-histogram, showing four distinct populations. Right: FCS analysis for selected bursts (autocorrelation with $I_1 = I_2 = I_A^{D\text{ex}} + I_D^{D\text{ex}}$), showing a different diffusion time for high- and low-FRET populations due to their different hydrodynamic radius. **c:** E-histograms of selected bursts ($0.2 < S < 0.8$). A low FRET population can clearly be observed for all three labeling positions. The low FRET population is 38 % for X and Z, and 10 % for Y, indicating progressive and pronounced nucleosome unwrapping from both ends. (Reprinted from [42], Copyright 2007, with permission from Elsevier.)

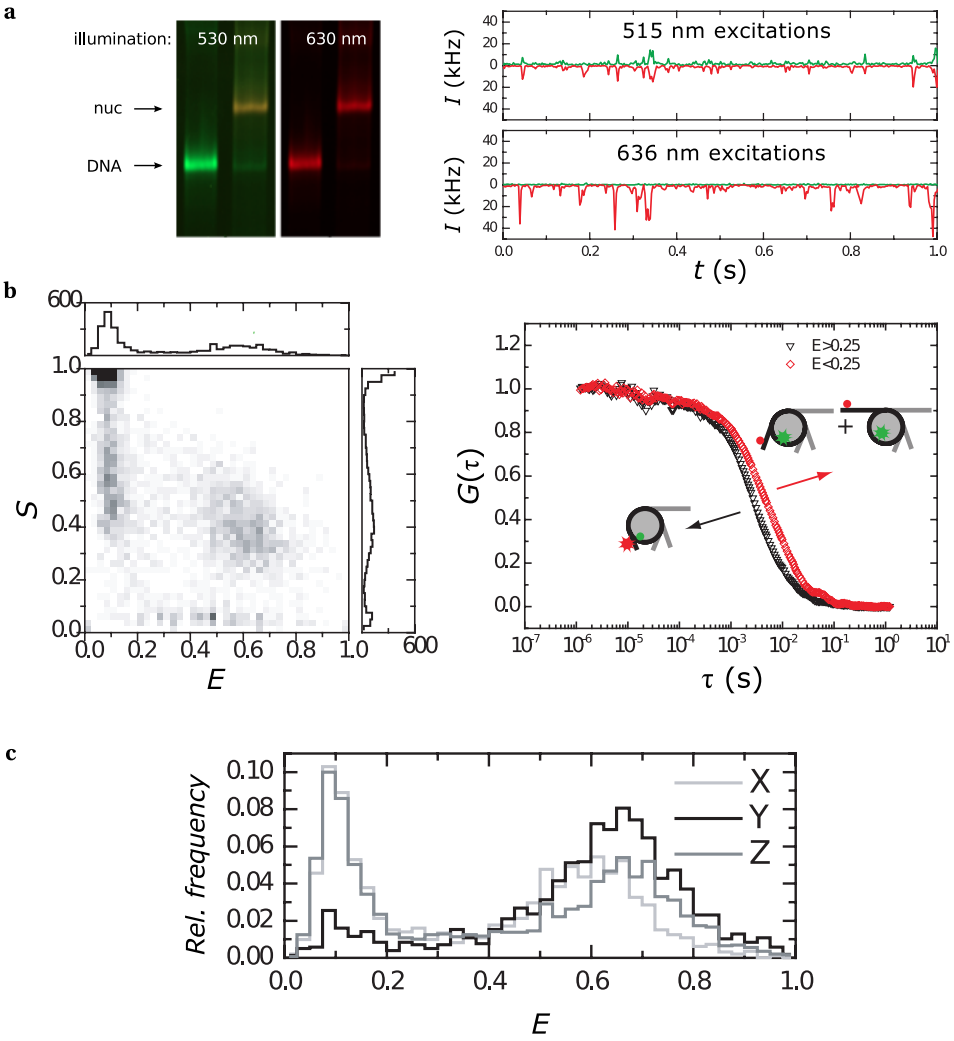
a
illumination:
530 nm
630 nm
nuc
DNA
515 nm excitations
636 nm excitations
I (kHz)
t (s)
b
S
E
G(τ)
τ (s)
E>0.25
E<0.25
c
Rel. frequency
X
Y
Z
E

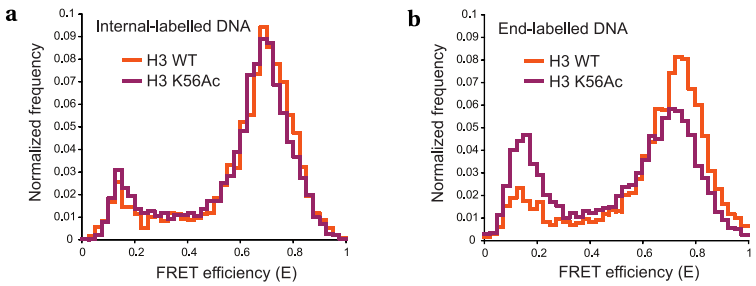

Figure 1.11 – *E*-histograms for nucleosomes with unmodified histones (H3 WT, orange) and histones acetylated at H3 K56 (H3 K56Ac, purple). Nucleosomes with the FRET labels at position X (**a**) and at position Y (**b**) (see figure 1.4f). The increase of the low-FRET population and the shift of the high-FRET population to a slightly lower FRET efficiency for the end-labeled nucleosomes shows that acetylation at H3 K56 promotes unwrapping of the first ~ 30 bp of the nucleosomal DNA. (Reprinted from [50] Copyright 2009, with permission from Elsevier.)

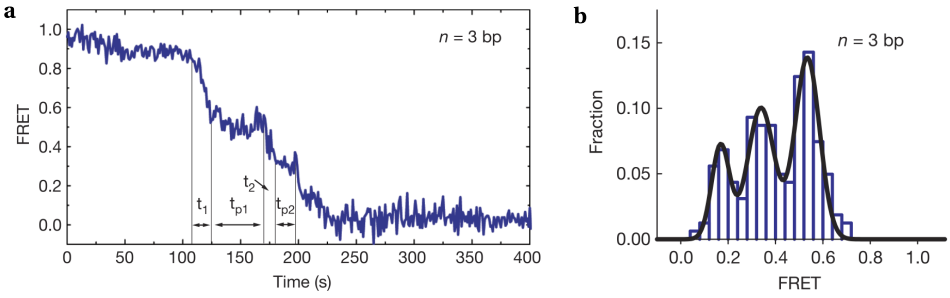

Figure 1.12 – ACF-catalyzed translocation of a single nucleosome. **a:** FRET time trace of an immobilized nucleosome after addition of ACF and ATP at t=0, showing kinetic pauses; **b:** FRET distribution of the pauses from time traces of many nucleosomes, revealing well-defined pauses. (Adapted by permission from Macmillan Publishers Ltd: Nature [51] copyright 2009.)

FRET due to nucleosome remodeling with a donor on the DNA and an acceptor on one of the histones [52]. They measured the ensemble donor or acceptor fluorescence intensity with a time resolution of 1 s during 6 minutes after activation of a SNF2h remodeler by adding ATP. Their nucleosome design is applicable to single-molecule experiments as well.

Blosser et al. recently reported the remodeling of nucleosomes by individual ACF complexes (ATP-dependent chromatin assembly and remodeling factor) [51] (label positions as in figure 1.4a, with D and A interchanged). With spFRET they directly monitored remodeling by ACF on individual immobilized nucleosomes. FRET-pair-labeled nucleosomes that initially show a high FRET signal gradually lose FRET when the histone octamer is repositioned with respect to the DNA by ACF. Translocation by ACF pauses at regular intervals of 7 or 3-4 bp (see figure 1.12). The binding, translocation, and dwell times of ACF are all ATP-dependent, revealing distinct roles of ATP during remodeling. It was also shown that ACF is highly processive, and can move nucleosomes in both directions along DNA before dissociating from the nucleosome.

1.10 DNA accessibility in nucleosome arrays

Restriction enzyme accessibility studies by Poirier et al. on longer arrays [53] surprisingly show that similar enzymatic accessibility to nucleosomal DNA can be observed in the arrays compared to mononucleosomes. Nucleosome positioning dramatically influences the accessibility of target sites inside nucleosomes, while chromatin folding dramatically regulates access to target sites in linker DNA between nucleosomes.

Though single nucleosomes provide excellent substrates to study DNA dynamics, *in vivo* nucleosomes always exist in the context of chromatin. In a combined bulk FRET, stopped flow, and FCS study, Poirier et al. quantified DNA accessibility in nucleosomal arrays [54] (figure 1.13). In this work, conformational dynamics of array compactness and site exposure inside the central nucleosome are probed on arrays of three nucleosomes. Bulk FRET and protein binding assays show that proteins can bind to sites in the central nucleosome of a compacted array, driven by site exposure in the central nucleosome, with rather similar kinetics to these of a single nucleosome. Array dynamics was probed on a construct where the DNA on the first and the third nucleosome was labeled. In this way, a high FRET signal is obtained when the array compacts, induced by adding Mg^{2+}. FRET-FCS and stopped-flow FRET analysis show that the short arrays show rapid spontaneous conformational dynamics and that protein binding can drive decompaction of the arrays. Based on these results, they propose a model for array dynamics with four different conformational states that have lifetimes ranging from microseconds to seconds. This study shows that spFRET has the potential to address structural dynamics beyond a single model nucleosome.

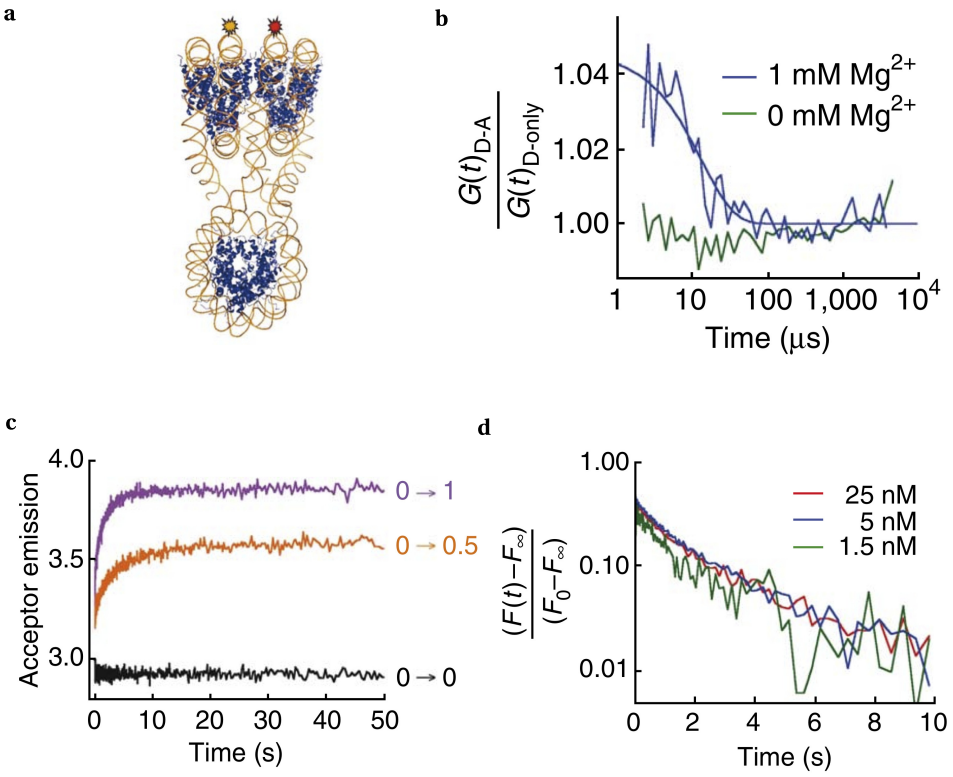

Figure 1.13 – Conformational dynamics of arrays of three nucleosomes. **a:** Three-nucleosomal construct; **b:** Ratio of the donor autocorrelation curves of a sample containing both labels and a donor-only sample isolates kinetics from diffusion fluctuations. Curves for compacted (blue) and extended (green) arrays. An exponential decay with a decay time of $\sim 10^{-5}$ s remains, indicating fluctuations between compact and less compact conformations on this timescale; **c:** stopped-flow FRET analysis of array compaction. Acceptor emission upon donor excitation during array compaction upon rapid mixing with Mg^{2+} (final concentrations 0, 0.5, or 1 mM) is followed. The large instantaneous increase in FRET indicates an array compaction on a timescale faster than $\sim 10^{-3}$ s (mixing dead time), while the further increase of compactness occurs on a timescale of ~ 2 s. **d:** Quantitative analysis of array compactness measured by FRET at different array concentrations. $F(t)$, F_0, and F^{∞}: acceptor fluorescence intensity at time (t), time 0 or at long times, respectively. Rate constants are independent of array concentration, ruling out aggregation effects. (Adapted by permission from Macmillan Publishers Ltd: Nature Structural and Molecular Biology [54] copyright 2009.)

1.11 Conclusions

Nucleosomes have been studied extensively by spFRET experiments. Restriction enzyme assays, bulk FRET and spFRET studies on mononucleosomes have revealed their conformation and dynamics. Here we have shown that despite experimental, instrumental, and biological differences employed in various studies, a coherent picture emerges of a dynamic nucleosome where spontaneous DNA breathing from the nucleosome ends provides access to the nucleosomal DNA. Nucleosomes are open 10 % of the time for tens of milliseconds. Nucleosome stability and DNA breathing can be modulated by DNA sequence and post-translational modifications of the histones. Translocation of nucleosomes along DNA by remodelers and conformational dynamics of higher order chromatin structures has been followed by spFRET. In the near future we can expect studies on more elaborate structures, that more closely resemble the *in vivo* chromatin organization. Integration of force spectroscopy and FRET will make the direct observation of dynamics under controlled force or torque conditions possible, conditions also established by the dynamic ensemble of many nucleosomes in the nucleus. When detailed mechanical behavior of mononucleosomes, arrays of two or a few nucleosomes, longer arrays, and the behavior of native chromatin in living cells have all been investigated, the combined data will provide the structural basis for epigenetic regulation mechanisms.